http://dx.doi.org/10.5012/bkcs.2012.33.1.221

Multiplexed DNA Detection with DNA-Functionalized Silver and Silver/Gold Nanoparticle Superstructure Probes

Ji-Young Kim and Jae-Seung Lee*

Department of Materials Science and Engineering, Korea University, Seoul 136-713, Korea
**E-mail: jslee79@korea.ac.kr*
Received October 20, 2011, Accepted November 21, 2011

DNA-functionalized silver and silver/gold bimetallic nanoparticle superstructure probes with controllable sizes and optical properties are synthesized using monothiol DNA and dithiothreitol. The superstructures exhibit a very narrow size distribution, which can be easily controlled by balancing the ratio of dithiothreitol and DNA. These superstructures assemble reversibly in a highly cooperative manner, and are SERS active. Multiplexed colorimetric detection of DNA targets using these superstructure probes has been demonstrated to identify three different DNA target sequences that are associated with three lethal diseases, respectively.

Key Words : DNA, SPR, Nanoparticle superstructure, Multiplexing, Colorimetric detection

Introduction

Sequence-specific detection of multiple DNA targets in parallel has long been an intensive focus of research such as disease diagnosis, forensic analysis, genomics, and biowarfare defence.[1] For this purpose, significant progress has been achieved in the area of DNA microarrays combined with molecular fluorophore probes, which is capable of analyzing a substantial number of oligonucleotides simultaneously.[2] This technology, however, requires precedent target amplification, lacks in ways to accelerate the target binding kinetics, has to consider photobleaching of fluorophores, and suffers from complicated, costly instrumentation, all of which have lead to the development of alternative advance based on metal nanoparticles, dendrimers, microspheres, porous photonic crystals, microrods, nanowires, and semiconductor nanoparticles.[3-12]

Plasmonic nanoparticle superstructures with defined sizes and shapes exhibit a variety of chemical and physical properties suitable as probes for molecular sensing.[13] As a building block of such superstructures, silver nanoparticles (AgNPs) are of particular interest owing to their intense optical properties based on surface plasmon resonance (SPR), electrochemical and catalytic activity, and strong Raman enhancement properties.[14-17] While a number of gold nanoparticle superstructures have been developed,[18-20] only a few reports have demonstrated the synthesis of AgNP superstructures (AgNP-SSs), often with limited functionalities, uncontrollable sizes and shapes, and irregular optical properties.[21-23] Based upon the excellent properties of individual AgNPs investigated for detecting a variety of targets,[24] the synthesis of AgNP-SS probes that are carefully designed to exhibit advanced properties would provide a new class of nanoprobes for efficient detection of multiple DNA targets.

Herein, we present the synthesis of DNA-conjugated AgNP-SS probes (DNA-AgNP-SS) for multiplexed colorimetric detection of DNA targets. To construct the stable and functional AgNP-SSs, we take advantage of the silver-sulfur covalent bonding formation to assemble the AgNPs into superstructures with controllable sizes and consequent optical properties using dithiol linker molecules, while monothiol DNA is used to inherently functionalize and stabilize the probes. By balancing the two types of thiol molecules, these novel structures exhibit easily controllable sizes and optical properties, target-recognizing surface functionalities, and SERS activities. Moreover, the reversible assembly properties of the AgNP-SSs associated with concomitant color changes are also attractive for building up further nano- and microstructure architectures.

Experimental Section

Materials. The eight HPLC-purified monothiol DNA sequences (**Ag-1**: 5' HS-A_{10}-ATTATCACT 3'; **Ag-2**: 5' HS-A_{10}-AGTGATAAT 3'; **A-1**: 5' TCCAACATTTACTCC-A_{10}-SH 3'; **A-2**: 5' HS-A_{10}-TTGTTGATACTGTTC 3'; **B-1**: 5' TTATTCCAAATATCTTCT-A_{10}-SH 3'; **B-2**: 5' HS-A_{10}-TGCATCCAGGTCATG 3'; **C-1**: 5' ATAAC-TGAAAGCC-AA-A_{10}-SH 3'; **C-2**: 5' HS-A_{10}-TACCACATCATCCAT 3') and the unmodified target DNA sequences (**A**: 5' GGAGTA-AATGTTGGAGAACAGTATCAACAA 3'; **B**: 5AGAAGA-TATTTGGAATAA-CATGACCTGGATGCA 3'; **C**: 5' TTG-GCTTTCAGTTATATGGATGATGTGGTA 3') were purchased from Genotech (Daejeon, Republic of Korea). The Cy5-labeled monothiol poly thymine (**RA**: 5 HS-Cy5-T_{20} 3) was purchased from Bioneer (Daejeon, Republic of Korea). Dithiothreitol (Cat.# 43815), gold chloride trihydrate (Cat.# 520918), trisodium citrate dihydrate (Cat.# S4641), and other chemicals for the buffer preparation were purchased from Sigma-Aldrich (Milwaukee, WI) and used without further purification. The NAP-5 sephadex column was purchased from GE Healthcare (Piscataway, NJ, USA). Silver nanoparticles (diameter: ~16 nm), Cat. # EM.SC20/7) were purchased from BBInternational (Cardiff, UK). Ultrapure

water from a Direct-Q3 system (18.2 MΩ cm, Millipore; Billerica, MA, USA) was used in this work.

Synthesis of Gold Nanoparticles (AuNPs). The aqueous solution of $HAuCl_4$ (0.254 mM, 50 mL) was boiled with vigorous stirring, and then reduced by injecting 0.94 mL of a 38.8 mM trisodium citrate solution quickly. The solution turned dark red from yellow. After the color change, the solution was kept boiling for additional 15 min and cooled to room temperature slowly. The diameter of the AuNPs was determined to be ~15 nm by transmission electron microscopy.

Synthesis of DNA-Silver Nanoparticle Superstructures (DNA-AgNP-SSs). The monothiol DNA sequences (Ag-1 and Ag-2) were deprotected with 0.10 M dithiothreitol (0.17 M phosphate buffer, pH 8.0), purified by a NAP-5 column, and adjusted to 20 mM in pure water. A series of concentrations of dithiothreitol (0, 1, 1.5, 2, 2.5, 2.8 and 3 mM, 10 uL) were injected to 225 uL of the DNA solution (20 μM), and further combined with 1 mL of AgNP solutions ([AgNP] = 2 nM), respectively (the final [DNA] = ~3.6 μM). The mixture solutions were further salt-adjusted to the final concentration of 0.15 M NaCl, 0.01% sodium dodecyl sulfate, and 10 mM phosphate (pH 7.4), resulting in color changes of the solutions due to the formation of DNA-AgNP superstructures with various sizes. After the incubation for a couple of hours, the unconjugated free DNA was removed from the solution by centrifugation of the superstructures (0: 14500 rpm; 1: 11000 rpm; 1.5: 9000 rpm; 2: 6000 rpm; 2.5: 2000 rpm; 2.8: 800 rpm; 3: 500 rpm, for 15 min), removal of the supernatant, and redispersion of the superstructures in buffer (0.15 M NaCl, 0.01% Tween 20, and pH 7.4, 10 mM phosphate).

Synthesis of DNA-Au/Ag Nanoparticle Superstructures (DNA-Au/AgNP-SSs). A mixture of the equal amount of gold and silver nanoparticles was used instead of silver nanoparticles for synthesis of DNA-Au/AgNP superstructures. A series of concentrations of dithiothreitol (0, 0.3, 0.4, 0.5 and 1 mM, 10 μL) were combined with 225 μL of the DNA solution (20 μM), and further combined with 1 mL of 1:1 mixture of silver and gold nanoparticles (total nanoparticle concentration was 2 nM), respectively (the final [DNA] = ~3.6 μM). The mixture solutions were further salt-adjusted in a same way of silver nanoparticle superstructures, and color changes of the solutions were also observed due to the formation of DNA-Au/AgNP superstructures. After the incubation for a couple of hours, the unconjugated free DNA was removed from the solution by centrifugation (0: 13000 rpm; 0.3: 11000 rpm; 0.4: 7000 rpm; 0.5: 6000 rpm; 1: 4000 rpm, for 20 min) and redipersed in buffer as described above.

UV-vis Spectroscopy Analysis. The optical properties of the both DNA-AgNP superstructures and DNA-Au/AgNP superstructures were characterized by the UV-vis spectroscopy from 230 to 1000 nm using an 8453 UV-vis Spectrophotometer (Agilent Technologies, Inc).

Melting Transition Experiments. The changes in extinction of DNA-AgNP superstructures and DNA-Au/AgNP superstructures at 260 nm were monitored at 1 °C interval at a rate of 1 °C/min from 25 °C to 70 °C to analyze melting transitions of the hybridized superstructures. The melting temperature (T_m) was obtained from the temperature where the maximum of the first derivative of the melting transition curve.

Dynamic Light Scattering Analysis. The series of both DNA-AgNP and DNA-Au/AgNP superstructures were characterized by dynamic light scattering analyzer (Nano ZS90, Malvern). A He-Ne gas laser provided incident light (beam wavelength: 632.8 nm) at the maximum output, 4 mW, and the scattered light from each sample was measured at a fixed angle of 90°. Five runs were performed, each with run duration of 15 s.

TEM Analysis of DNA-AgNP and DNA-Au/AgNP Superstructures. DNA-AgNP superstructures of four sizes ([DTT] = 1.0, 1.5, 2.0, and 2.5 mM) and DNA-Au/AgNP superstructures ([DTT] = 0.4 mM) were prepared for TEM analysis. Each sample (4 μL) was dropped onto a carbon-coated Formvar copper grid (400 mesh) and allowed to dry in a dust free area. TEM analyses were performed using a Tecnai 20 operating at 200 kV.

Synthesis of DNA-AgNP and DNA-Au/AgNP Superstructure Probes for Multiplexed Detection. Two sets of DNA-AgNP superstructure probes (1.0 and 2.5 DNA-AgNP superstructures, respectively) and a set of 1.0 DNA-Au/AgNP superstructure probe were used for multiplexed detection of target sequences **A**, **B**, and **C**. Each set of probes is synthesized with two types of sequences so as not to interact with each other, but assemble and form bigger aggregates when the complementary target sequence presents. The 1.0 DNA-AgNP superstructures were synthesized with two types of sequences (**A-1** and **A-2**) so as to react with target **A**. We also designed two other probes, 2.5 DNA-AgNP superstructures and 1.0 DNA-Au/AgNP superstructures, to react target **B** and **C** by functionalizing each with two types of sequence, respectively. (2.5 DNA-AgNP superstructures: **B-1** and **B-2**; 1.0 DNA-Au/AgNP superstructures: **C-1** and **C-2**).

Multiplexed Colorimetric Detection of Target DNA. To evaluate the colorimetric detection system for multiplex target sequences, eight aliquots were run with different combinations of the target DNA sequences, **A**, **B** and **C**. Eight batches of the mixture of the six probes (180 μL of each) were prepared in glass vials. In the first, blank (20 μL of phosphate buffer) was injected. In the next six tests, three targets were systematically combined to the probe solutions to evaluate the multiplexing capability of the probes. The concentration of the target DNA sequences were kept constant for all tests (50 nM of final concentration for each sequence). **A**, **B**, **C**, **A**+**B**, **A**+**C**, **B**+**C**, **A**+**B**+**C** target solutions (20 μL, 500 nM for each sequence) were respectively combined to the probes so as to be the final target concentration of 50 nM. All batches were kept at 25 °C for 36 hours. The optical signal corresponding to the target combinations were identically observed.

Synthesis of Cy5-Labeled DNA-AgNP and DNA-Au/

AgNP Superstructure Probes. We synthesized DNA-AgNP and 2.5 DNA-AgNP superstructure probes using Cy5-labeled monothiol DNA (**RA**: 5' HS-Cy5-T_{20} 3') SERS as described above.

SERS Measurement. SERS Raman spectra measurement of Cy5-labeled DNA-AgNP and DNA-AgNP superstructure probes were carried out using Nanofinder 30 (Tokyo Instruments, INC, Japan) having 633 nm HeNe laser. The probe solutions (100 μL each) were dropped onto a clean glass slide and covered with a cover slide. The liquid samples were kept under microscope objective lens for measurement and the Raman spectra were collected in the wave number range of 600-1750 cm^{-1}. Four runs were performed on each sample, with an exposure time of 60 s.

Results and Discussion

Scheme 1 describes our synthetic approach for the DNA-AgNP-SS probes. The AgNPs (D = 16 nm, 2 nM) are combined with a mixture of thiol DNA and dithiothreitol (DTT) whose concentrations vary depending upon the desired size and optical properties of the probe (see Experimental Section). To effectively control the superstructure size, the concentration of the DTT stock solution gradually increases from 0 to 3 mM, resulting in the color change of the superstructured AgNPs to orange, red, and purple (Fig. 1(a)). This color change was further analyzed by UV-vis spectroscopy, which demonstrates a systematic red-shift of λ_{MAX} from 403 to 578 nm with a decrease in extinction (Fig. 1(b)). Importantly, the extinction of the AgNP-SSs obtained with the highest [DTT] still remained at ~40% of the same number of individual AgNPs, indicating that the AgNP-SSs are composed to distinct number of AgNPs devoid of indefinite particle aggregation. To examine the versatility of the synthetic method, we also synthesized DNA-conjugated Au/Ag bimetallic superstructures (DNA-Au/Ag-SSs) using

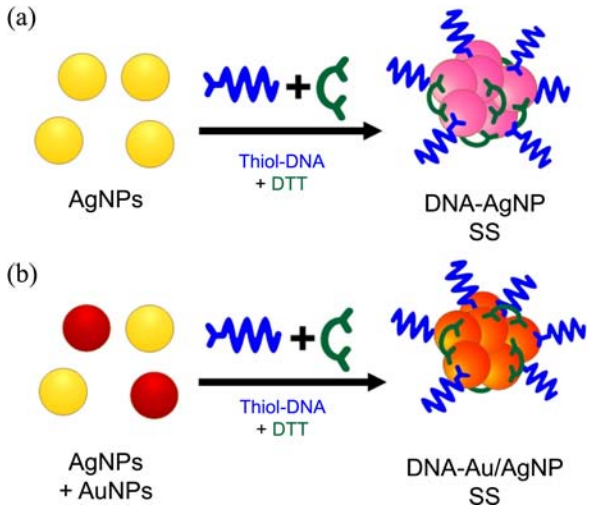

Scheme 1. A scheme illustrating the synthesis of DNA-functionalized (a) silver nanoparticle superstructure (DNA-AgNP-SS) probes and (b) bimetallic gold/silver nanoparticle superstructure (DNA-Au/AgNP-SS) probes.

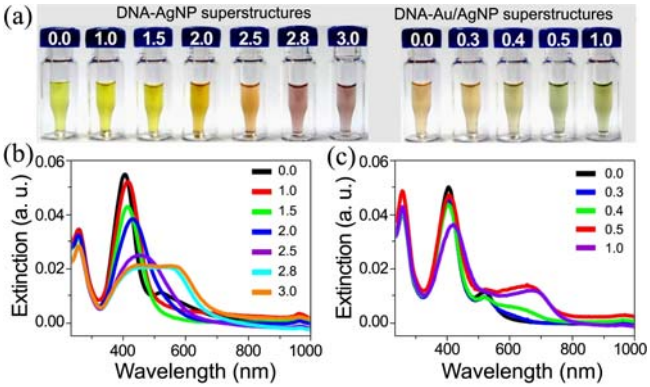

Figure 1. (a) DNA-functionalized silver nanoparticle superstructures (DNA-AgNP-SSs) and gold/silver bimetallic superstructures (DNA-Au/AgNP-SSs). The DTT concentrations used for the synthesis are labelled on the cap of the vials (see Experimental Section). (b) UV-vis spectra of DNA-AgNP-SSs and (c) DNA-Au/AgNP-SSs. The numbers in the legend indicate the DTT concentrations used for the synthesis (see Experimental Section).

equal number of gold nanoparticles (AuNPs) and AgNPs, which exhibited a variety of chromatic diversity from orange to green (Fig. 1(a)) and associated spectra (Fig. 1(c)). It is notable that unlike the DNA-AgNP-SSs, the λ_{MAX} of the DNA-Au/AgNP-SSs only decreased in extinction without any significant spectral shift, while a new plasmon began to appear at ~670 nm, which is analogous to superstructures composed of only AuNPs.[18]

To confirm the defined sizes of these superstructures, we analyzed the diameter of the AgNP-SSs using dynamic light scattering (DLS). As we increased the [DTT], the diameter of the DNA-AgNP-SSs increased from ~23 up to ~500 nm

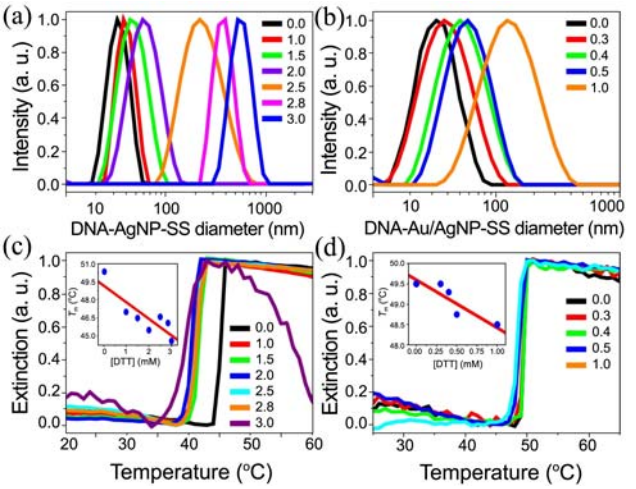

Figure 2. (a) The size distribution of the DNA-AgNP-SSs and (b) DNA-Au/Ag-SSs were measured by dynamic light scattering (DLS). The single and narrow peaks indicate that the superstructures are well monodispersed. (c) Normalized melting transitions of the assembled DNA-AgNP-SSs and (d) DNA-Au/AgNP-SSs with various sizes. The insets show the melting temperatures (T_ms) as a function of the [DTT]. The T_ms were determined by the first derivative of the melting transitions. The numbers in the legend indicate the DTT concentrations used for the synthesis (see Experimental Section).

with very narrow size distributions (Fig. 2(a)). The DNA-Au/AgNP-SSs exhibited slightly broader size distributions, but still systematically increasing diameters as a function of [DTT] (Fig. 2(b)). Importantly, the monodispersity of these probes is essential for their quantitative and analytical applications from the diagnostic viewpoint. Subsequently, we evaluated the DNA-functionality of the superstructure probes by combining two complementary DNA-AgNP-SS and DNA-Au/Ag-SS probes for hybridization, respectively, and conducting thermal denaturation experiments to obtain their melting profiles (Fig. 2(c) and (d)). When combined, both types of superstructure probes rapidly hybridized to form macroscopic aggregates with concomitant color changes. These aggregates, however, reversibly disassembled into the original superstructures with very sharp melting transition curves (full width at half maximum = ~2.2 °C), indicating these DNA-AgNP-SS and Au/Ag-SS probes are densely functionalized with DNA.[10] Interestingly, the melting temperature (T_m) of each melting transition decreased as the superstructure size increased with negative correlations (Fig. 2(c) and (d), inset), which is opposite to the positive correlations between size and T_m of individual DNA-nanoparticle conjugate probes.[25,26] We attribute these decreases in T_m to (1) the non-spherical shape of the superstructures and (2) their size-dependent negative charges. Being assemblies of nanoparticles, the surface of the superstructure is uneven and rough. Unlike individual nanoparticle probes, therefore, the probe-probe contact area which is associated with the number of DNA strands involving in hybridization of the superstructure probes would not be directly proportional to the superstructure size. Meanwhile, the increasing negative charge owing to the more DNA strands of larger superstructure would lead to more repulsion, resulting in decreasing T_m.

The increasing size of the DNA-AgNP-SSs were observed by transmission electron microscopy (TEM) and shown in Figure 3. The first four DNA-AgNP-SSs were selected and analyzed. With the [DTT] from 1 to 2.5 mM, the increase in size of the AgNP-SSs was clearly observed (Fig. 3(a)-(d)) up to 250 nm. Meanwhile, the overall shape evolved from isotropically assembled nanoparticles to form fractal-like structures as previously proposed by theory.[27] In addition, to verify that the DNA-Au/AgNP-SSs were composed of both Au and AgNPs, we analyzed several selected areas of a bimetallic superstructure using TEM and energy-dispersive X-ray spectroscopy (EDS) (Fig. 3(e), (f), (g), (h), and (i)).

Based on the optical, functional, and assembly properties of the superstructure probes, we conducted the multiplexed detection of three DNA targets (**A**, **B**, and **C**) that are sequences of 30 to 33 bases associated with Ebola virus (**A**), human immunodeficiency virus (**B**), and hepatitis B virus surface-antigen gene (**C**) as model systems (see Experimental Section). Three pairs of superstructure probes with distinctive optical properties were prepared such that two types of DNA-AgNP-SSs with 1.0 mM DTT are complementary to each half of **A**, DNA-AgNP-SSs with 2.5 mM DTT to each half of **B**, and DNA-Au/AgNP-SSs with 1.0 mM DTT to each half of **C** (see Experimental Section). Before the hybridization reaction of the probes with target sequences, aliquots of the mixtures exhibited dark but intense yellow color (Fig. 4(a)). When combined with all eight possible combinatorial cases of the target mixtures (blank, A+B, A+C, B+C, A, B, C, and A+B+C, 50 nM each), however, the superstructure probes in each mixture began to rapidly hybridize with corresponding targets to form reversible assemblies. The functional DNA sequences on the superstructure probes selectively recognize the specific target sequences, resulting in the distinctive color changes depending on the combination of the targets (Fig. 4(b)). The 'blank' mixture retained the initial color, while the probes in the presence of all the targets completely hybridized to form large assemblies, leading to the colorless, clear solution. The other target combinations between them exhibit various colors ranging from red (**B**+**C**) to green (**A**+**C**). Importantly, the unique resultant color of each mixture can be considered as an optical signature to indicate the types of the target sequences.

We finally evaluated the surface enhanced Raman scattering (SERS) activity of the DNA-AgNP-SS probes and compared them with individual AgNP probes. We designed a DNA sequence containing a thiol group next to a Raman dye (Cy5) in one end of polythymine (T_{20}), and labelled AgNP-SS ([DTT] = 2.5 mM) and AgNP probes with the sequence. Both types of probes were examined by Raman

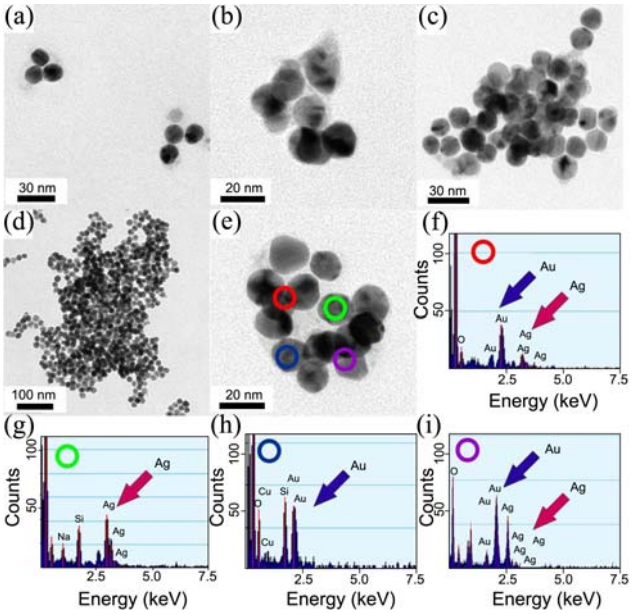

Figure 3. TEM images of the DNA-AgNP-SSs with [DTT] = (a) 1.0 mM, (b) 1.5 mM, (c) 2.0 mM, (d) 2.5 mM, and (e) DNA-Au/AgNP-SSs with [DTT] = 0.4 mM. (f) The selected TEM area within the red circle in (3) was analyzed by energy-dispersive X-ray spectroscopy (EDS), whose spectrum exhibits the peaks for both gold and silver. (g) The EDS spectrum for the selected area within the green circle in (3) exhibits the peaks for silver only. (h) The EDS spectrum for the selected area within the blue circle in (3) exhibits the peaks for gold only. (i) The EDS spectrum for the selected area within the purple circle in (3) exhibits the peaks for both gold and silver.

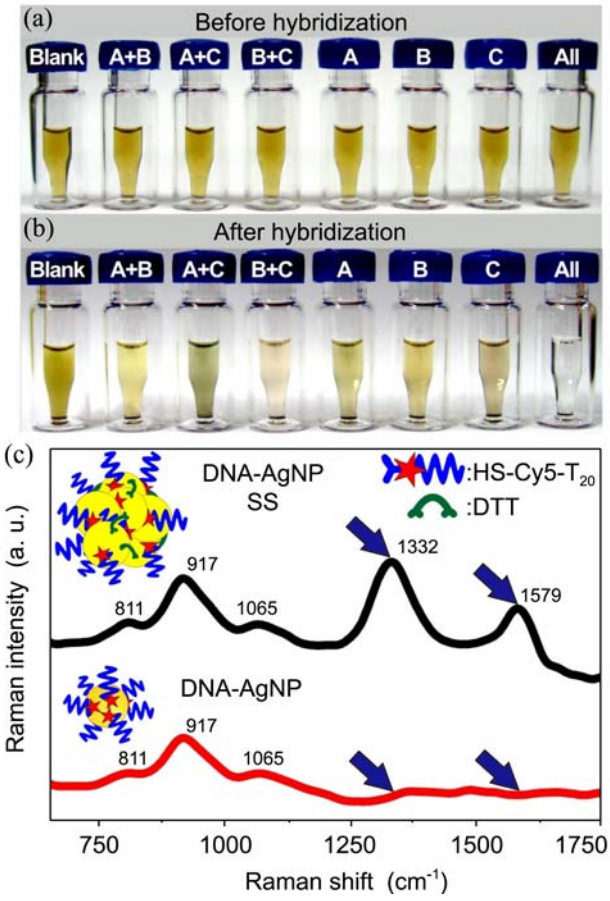

Figure 4. Mixed superstructure probes with various combinations of targets (a) before hybridization and (b) after hybridization. (c) SERS spectra of DNA-AgNP-SSs and DNA-AgNPs, each labelled with Cy5.

spectroscopy, whose spectra were collected in the wave number range of 600-1750 cm^{-1} (see Experimental Section) (Fig. 4(d)). While both probes exhibited three major bands at 811, 917 and 1065 cm^{-1} in common, the dramatically improved SERS activity of the AgNP-SS probes was observed with the characteristic bands at 1332 and 1579 cm^{-1}. This result matches well with the previous literature results.[28,29] Interestingly, however, we were not able to observe any SERS enhancement at 1332 and 1579 cm^{-1} with the Au/AgNP-SS probes. In fact, the SERS signals of Raman dyes on atomically alloyed gold-silver nanoparticles are known to be affected by the shape and composition of the particles.[30] Considering that our superstructures are extensions of such alloy nanoparticles where a nanoparticle is corresponding to an atom, potential destructive interference of the electromagnetic field around the DNA-Au/AgNP-SSs could be the reason for their SERS inactivity. Further research to investigate the SERS inactivity of the DNA-Au/AgNP-SSs is ongoing. Considering that typical core-shell type gold/silver bimetallic nanostructures and even pure silver nanomaterials exhibit characteristic SERS activity,[31-34] our results indicate that both the elemental composition and assembly structure of nanoparticles have considerable effects on Raman enhancement.

Conclusion

We have synthesized silver and gold/silver nanoparticle superstructures with controlled sizes, distinctive SPR- and SERS-based optical properties, and target-specific DNA-functionalities for the colorimetric multiplexed detection of DNA targets. The size of the superstructures exhibit a very narrow distribution, which can be easily controlled by the stoichiometry of a crosslinking reagent (dithiothreitol) and monothiol DNA. These superstructures assemble reversibly in a highly cooperative manner. In particular, the silver nanoparticle superstructures exhibit strong SERS activity. We further demonstrated the multiplexed colorimetric detection of DNA targets using these superstructure probes to identify three different DNA target sequences that are associated with three lethal diseases, respectively. Significantly, the reversible assembly formation of the superstructures provides an important strategy to systematically build up giant structures of nanomaterials in a hierarchical manner using DNA. Moreover, our novel synthetic method could be extended for other bimetallic, or further complicated multimetallic nanoparticle superstructures with controllable size and stoichiometry, which would offer deeper insights into the properties of assembled nanostructures, especially as conceptual expansion of the conventional atomically alloyed nanomaterials.

Acknowledgments. This work was supported by the 2nd stage of the Brain Korea 21 Project in 2011, and Basic Science Research Program through the National Research Foundation of Korea (NRF) funded by the Ministry of Education, Science and Technology (Grant No. 2011-0027400).

References

1. Lockhart, D. J.; Winzeler, E. A. *Nature* **2000**, *405*, 827.
2. Niemeyer, C. M.; Blohm, D. *Angew. Chem., Int. Ed.* **1999**, *38*, 2865.
3. Li, Y.; Cu, Y. T. H.; Luo, D. *Nat. Biotechnol.* **2005**, *23*, 885.
4. Han, M.; Gao, X.; Su, J. Z.; Nie, S. *Nat. Biotechnol.* **2001**, *19*, 631.
5. Zhao, X.; Tapec-Dytioco, R.; Tan, W. *J. Am. Chem. Soc.* **2003**, *125*, 11474.
6. Cunin, F.; Schmedake, T. A.; Link, J. R.; Li, Y. Y.; Koh, J.; Bhatia, S. N.; Sailor, M. J. *Nat. Mater.* **2002**, *1*, 39.
7. Nicewarner-Pena, S. R.; Freeman, R. G.; Reiss, B. D.; He, L.; Pena, D. J.; Walton, I. D.; Cromer, R.; Keating, C. D.; Natan, M. J. *Science* **2001**, *294*, 137.
8. Cui, Y.; Wei, Q.; Park, H.; Lieber, C. M. *Science* **2001**, *293*, 1289.
9. Mirkin, C. A.; Letsinger, R. L.; Mucic, R. C.; Storhoff, J. J. *Nature* **1996**, *382*, 607.
10. Niemeyer, C. M.; Simon, U. *Eur. J. Inorg. Chem.* **2005**, 3641.
11. Wang, J.; Liu, G.; Merkoci, A. *J. Am. Chem. Soc.* **2003**, *125*, 3214.
12. Stoeva, S. I.; Lee, J.-S.; Thaxton, C. S.; Mirkin, C. A. *Angew. Chem., Int. Ed.* **2006**, *45*, 3303.
13. Tan, S. J.; Campolongo, M. J.; Luo, D.; Cheng, W. L. *Nat. Nanotechnol.* **2011**, *6*, 268.
14. Link, S.; Wang, Z. L.; El-Sayed, M. A. *J. Phys. Chem. B* **1999**,

103, 3529.
15. Jiang, Z.-J.; Liu, C.-Y.; Sun, L.-W. *J. Phys. Chem. B* **2005**, *109*, 1730.
16. Braun, G.; Lee, S. J.; Dante, M.; Nguyen, T.-Q.; Moskovits, M.; Reich, N. *J. Am. Chem. Soc.* **2007**, *129*, 6378.
17. Sun, L. L.; Zhao, D. X.; Ding, M.; Xu, Z. K.; Zhang, Z. Z.; Li, B. H.; Shen, D. Z. *J. Phys. Chem. C* **2011**, *115*, 16295.
18. Kim, J.-Y.; Lee, J.-S. *Nano Lett.* **2009**, *9*, 4564.
19. Chen, C. L.; Rosi, N. L. *J. Am. Chem. Soc.* **2010**, *132*, 6902.
20. Hwang, L.; Zhao, G. P.; Zhang, P. J.; Rosi, N. L. *Small* **2011**, *7*, 1939.
21. Tao, A. R.; Ceperley, D. P.; Sinsermsuksakul, P.; Neureuther, A. R.; Yang, P. D. *Nano Lett.* **2008**, *8*, 4033.
22. Graham, D.; Thompson, D. G.; Smith, W. E.; Faulds, K. *Nat. Nanotechnol.* **2008**, *3*, 548.
23. Hulteen, J. C.; Treichel, D. A.; Smith, M. T.; Duval, M. L.; Jensen, T. R.; Van Duyne, R. P. *J. Phys. Chem. B* **1999**, *103*, 3854.
24. Thompson, D. G.; Enright, A.; Faulds, K.; Smith, W. E.; Graham, D. *Anal. Chem.* **2008**, *80*, 2805.
25. Jin, R.; Wu, G.; Li, Z.; Mirkin, C. A.; Schatz, G. C. *J. Am. Chem. Soc.* **2003**, *125*, 1643.
26. Lee, J.-S.; Stoeva, S. I.; Mirkin, C. A. *J. Am. Chem. Soc.* **2006**, *128*, 8899.
27. Park, S. Y.; Lee, J. S.; Georganopoulou, D.; Mirkin, C. A.; Schatz, G. C. *J. Phys. Chem. B* **2006**, *110*, 12673.
28. Malvadkar, N. A.; Demirel, G.; Poss, M.; Javed, A.; Dressick, W. J.; Demirel, M. C. *J. Phys. Chem. C* **2010**, *114*, 10730.
29. Faulds, K.; Smith, W. E.; Graham, D. *Anal. Chem.* **2004**, *76*, 412.
30. Cui, Y.; Ren, B.; Yao, J. L.; Gu, R. A.; Tian, Z. Q. *J. Phys. Chem. B* **2006**, *110*, 4002.
31. Hunyadi, S. E.; Murphy, C. J. *J. Mater. Chem.* **2006**, *16*, 3929.
32. Rivas, L.; Sanchez-Cortes, S.; Garcia-Ramos, J. V.; Morcillo, G. *Langmuir* **2000**, *16*, 9722.
33. Lim, D. K.; Jeon, K. S.; Kim, H. M.; Nam, J. M.; Suh, Y. D. *Nat. Mater.* **2010**, *9*, 60.
34. Lim, D. K.; Jeon, K. S.; Hwang, J. H.; Kim, H.; Kwon, S.; Suh, Y. D.; Nam, J. M. *Nat. Nanotechnol.* **2011**, *6*, 452.